

Study of the Dispersive Contribution Effect for Neutrons Scattering by ^{60}Cu Nucleus Using Variational Moment Approach

Molhum Ussef, Anees Belal

Department of Physics, Faculty of Science, Al-Baath University, Homs, Syria

Email address:

Molhuma3@gmail.com (M. Usef), aneesblaldr@gmail.com (A. Belal)

To cite this article:

Molhum Ussef, Anees Belal. Study of the Dispersive Contribution Effect for Neutrons Scattering by ^{60}Cu Nucleus Using Variational Moment Approach. *Nuclear Science*. Vol. 5, No. 4, 2020, pp. 44-49. doi: 10.11648/j.ns.20200504.11

Received: November 18, 2020; **Accepted:** December 23, 2020; **Published:** December 31, 2020

Abstract: The variational moment approach for the neutrons scattering analysis by ^{60}Cu nucleus within the energy range (60-80) MeV is applied to the construction of the complex single-particle mean field felt by neutrons in ^{60}Cu , starting from negative energy values to the positive energy values. The experimental data of the scattering neutron has been analysis by using one of the methods for optical dispersion model which depending on the afferent between the real and imaginary parts and this led to a derivation decrease in determining the optical parameters from the experimental data. Also on the stripe expanding of the real potential parameters from high energy to low energy to the close area of the Coulomb barrier which characterized the lack of information about the experimental data for each, using the program SPI-GINOA in order to determine the value of the volume integral for the real and imaginary parts (surface and volume). The Value of the volume integral for the real part and integrals oh "Hartree – Fock" was pointed and then determined the value of real part of the potential Hartree – fock potential. In addition we also has been determined the imaginary potential (two parts the surface and the volume) and studied on function of energy for all the specific pointed ingredients. The potential dispersion was determined (surface – volume) and studied their functional energy. Therefore, we determined the radius neutron optical model and also we found its energy way match close to what reveal the correctness of method of dispersive optical model at one hand, and the accuracy in the determination of optical model parameters at other hand.

Keywords: Variational Moment Approach (VMA), Dispersion Relations (DR), Total Cross Section, Neutrons Scattering, Optical Neutron Potential, Mean Field, Fermi Energy

1. Introduction

The nuclear optical model potential is of the fundamental importance concepts in the nuclear physics. It describes the motion of one nucleon, bound or unbound, in the mean field of all the other nucleons comprising the nucleus. The field due to the sum of all the individual nucleon-nucleon interactions is thus represented by a simple one-body potential. This approximation greatly simplifies the calculation of a wide range of nuclear structure and nuclear reaction phenomena, in addition to the excellent agreement with experimental data [1]. The application of the concept of the nuclear mean field is for understanding the properties of bound single-particle states and for elastic scattering of unbound nucleons [1-3].

The phenomenological optical model potential for nucleon-nucleus scattering, U , is defined as [2-8]:

$$U(r, E) = -V_V(r, E) - V_{SO}(r, E) \cdot \vec{\sigma} \cdot \vec{l} + V_d(r, E) + V_C(r) + i(-W_V(r, E) - W_d(r, E) + W_{SO}(r, E) \cdot \vec{\sigma} \cdot \vec{l}) \quad (1)$$

Where $V_{V,S}$ and $W_{V,S,SO}$ are the real and imaginary components of the volume-central (V), surface-central (d) and spin-orbit (SO) potentials, respectively. E is the LAB energy of the incident particle in MeV . All components are separated in energy-dependent well depths, $V_V, V_d, V_{SO}, W_V, W_d$ and W_{SO} , and energy-independent radial parts f , namely

$$\begin{aligned}
V_V(r,E) &= V_V(E)f(r,R_V,a_V) \\
W_V(r,E) &= W_V(E)f(r,R_V,a_V) \\
W_d(r,E) &= -4a_d W_d(E) \frac{d}{dr} f(r,R_d,a_d) \\
V_d(r,E) &= -4a_d V_d(E) \frac{d}{dr} f(r,R_d,a_d) \\
V_{SO}(r,E) &= V_{SO}(E) \left(\frac{\hbar}{m\pi c}\right)^2 \frac{1}{r} \frac{d}{dr} f(r,R_{SO},a_{SO}) \\
W_{SO}(r,E) &= W_{SO}(E) \left(\frac{\hbar}{m\pi c}\right)^2 \frac{1}{r} \frac{d}{dr} f(r,R_{SO},a_{SO})
\end{aligned} \quad (2)$$

The form factor $f(r, R_i, a_i)$ is a Wood-Saxon shape

$$f(r, R_i, a_i) = \frac{1}{[1 + e^{\frac{r-R_i}{a_i}}]} \quad (3)$$

Where the geometry parameters are the radius $R_i = r_i A^{\frac{1}{3}}$, with A the atomic mass number, and the diffuseness parameters $a_i, i = V, SO, d$. For neutrons scattering, the value of the coulomb term V_C , is zero.

By solving the Schrödinger equation numerically with this complex potential yields a wealth of valuable information; it returns a prediction for the basic observables, namely the elastic angular distribution and the reaction and total cross section [4-8].

The present paper aims at presenting the variational moment approach (VMA) of the neutrons scattering by ^{60}Cu nucleus and comparing the results with these resulting from global parametrization of the optical model potential and available experimental data within energy range (60-80) MeV and its extend to the reliable low and high energy domain from the studied energy range according to evaluated fitting methodology.

2. Methodology

The methodology of (VMA) is summarized as follows [2-4, 7-10]:

2.1. Volume Integral Per Nucleon

Determining the continuous energy variation of the volume integral per nucleon by using Brown-Rho (Br) expression:

For the central imaginary part of the nuclear mean field:

$$[r^2]_W(E) = \beta \frac{(E-E_0)^2}{(E-E_0)^2 + \rho_W^2} \quad (4)$$

The imaginary part has a volume and a surface component, the volume component is,

$$[r^2]_{W_V}(E) = \beta \frac{(E-E_0)^2}{(E-E_0)^2 + \rho_{W_V}^2} \quad (5)$$

So, the surface component is,

$$[r^2]_{W_d}(E) = [r^2]_W(E) - [r^2]_{W_V}(E) \quad (6)$$

where $\beta, \rho_W, \rho_{W_V}$ denote Brown-Rho parameters, E_0 is:

$$E_0 = \frac{E_F}{2} \quad (7)$$

Where, E_F , the Fermi energy in MeV, that is defined as the energy halfway between the last occupied and the first

unoccupied shell of the nucleus, determined from the experimental masses as follows[13]:

$$\begin{aligned}
E_F &= \frac{E_F^+ + E_F^-}{2} \\
E_F^+ &= M_{A+1} - M_A - m \\
E_F^- &= M_A - M_{A-1} - m
\end{aligned} \quad (8)$$

Where E_F^+ is the negative of the separation energy of a nucleon from the $(A+1)$ -nucleon system. Also, E_F^- is the negative of the separation energy of a nucleon from the A -nucleon system, m is the atomic mass of the incident particle.

2.2. Depths of the Volume and Surface Absorption of the Mean Field

Determining the continuous energy variation of the volume and surface absorption depths,

$$W_V(E) = [r^2]_{W_V}(E) / g_{wv}, \text{ MeV} \quad (9)$$

$$W_d(E) = [r^2]_{W_d}(E) / g_{wd}, \text{ MeV} \quad (10)$$

Where g_{wv}, g_{ws} can be written as follows:

$$g_{wv} = \frac{4\pi}{3} \frac{R_{wv}^3}{A_t * A_p} \left[1 + \left(\frac{\pi a_{wv}}{R_{wv}} \right)^2 \right] \quad (11)$$

$$g_{wd} = \frac{16\pi R_{wd}^2 a_{wd}}{A_t * A_p} \left[1 + \frac{1}{3} \left(\frac{\pi a_{wd}}{R_{wd}} \right)^2 \right] \quad (12)$$

Where $R_{wv} = r_{wv} A_t^{\frac{1}{3}}$, a_{wv} , $R_{wd} = r_{wd} A_t^{\frac{1}{3}}$, a_{wd} are the radius and diffuseness parameters of the volume and surface absorption.

2.3. Volume Integral Per Nucleon of Dispersive Corrections of the Real Part of the Mean Field

The dispersion relations are a natural result of the causality principle that a scattered wave cannot be emitted before the arrival of the incident wave. The dispersion component stems directly from the absorptive part of the potential,

$$\Delta \mathcal{V}(r, E) = \frac{\mathcal{P}}{\pi} \int_{-\infty}^{+\infty} \frac{\mathcal{W}(r, E')}{E' - E} dE' \quad (13)$$

Where \mathcal{P} denotes the principal value. The total real central potential can be written as the sum of a Hatree-Fock term $\mathcal{V}_{HF}(r, E)$ and the total dispersion potential $\Delta \mathcal{V}(r, E)$

$$\mathcal{V}(r, E) = \mathcal{V}_{HF}(r, E) + \Delta \mathcal{V}(r, E) \quad (14)$$

Since $\mathcal{W}(r, E)$ has a volume and a surface component, the dispersive addition is,

$$\begin{aligned}
\Delta \mathcal{V}(r, E) &= \Delta \mathcal{V}_V(r, E) + \Delta \mathcal{V}_d(r, E) \\
&= \Delta \mathcal{V}_V(E) f(r, R_V, a_V) - 4a_d \Delta \mathcal{V}_d(E) \frac{d}{dr} f(r, R_d, a_d)
\end{aligned} \quad (15)$$

Where the volume dispersion term is given by

$$\Delta \mathcal{V}_V(E) = \frac{\mathcal{P}}{\pi} \int_{-\infty}^{+\infty} \frac{W_V(E')}{E' - E} dE' \quad (16)$$

And the surface dispersion term is given by

$$\Delta V_D(E) = \frac{\mathcal{P}}{\pi} \int_{-\infty}^{+\infty} \frac{W_D(E')}{E' - E} dE' \quad (17)$$

In general, “(16)” & “(17)” cannot be solved analytically. However, under certain plausible conditions, analytical solutions exist. Under the assumption that the imaginary potential is symmetric with respect to the Fermi energy E_F

$$W(E_F - E) = W(E_F + E) \quad (18)$$

Where W denotes either the volume or surface term, we can rewrite the dispersion relation as,

$$\Delta V(E) = \frac{2}{\pi} (E - E_F) \mathcal{P} \int_{E_F}^{\infty} \frac{W(E')}{(E' - E_F)^2 - (E - E_F)^2} dE' \quad (19)$$

Determining the continuous energy variation of the volume integral per nucleon of dispersive corrections of the real part of the mean field is obtained by using the dispersion relations:

The total dispersive correction:

$$[r^2]_{\Delta V_W}(E) = \frac{2}{\pi} (E - E_F) \int_{E_0}^{\infty} \frac{[r^2]_W(E')}{(E' - E_F)^2 - (E - E_F)^2} dE' \quad (20)$$

The volume dispersive correction:

$$[r^2]_{\Delta V_{WV}}(E) = \frac{2}{\pi} (E - E_F) \int_{E_0}^{\infty} \frac{[r^2]_{WV}(E')}{(E' - E_F)^2 - (E - E_F)^2} dE' \quad (21)$$

So, the surface dispersive correction is:

$$[r^2]_{\Delta V_{Wd}}(E) = [r^2]_{\Delta V_W}(E) - [r^2]_{\Delta V_{WV}}(E) \quad (22)$$

2.4. Depths of the Dispersive Corrections of the Real Optical Potential

Determining the continuous energy variation of the depths of the dispersive corrections of the real optical potential:

The volume dispersive correction:

$$\Delta V_V(E) = [r^2]_{\Delta V_{WV}}(E) / g_{wv}, \text{ MeV} \quad (23)$$

The surface dispersive correction:

$$\Delta V_d(E) = [r^2]_{\Delta V_{Wd}}(E) / g_{wd}, \text{ MeV} \quad (24)$$

So, the total dispersion potential $\Delta \mathcal{V}(r, E)$ calculated from “(15)”, at $r = 0$.

2.5. Depth of the Total Real Central Potential

Determining the continuous energy variation of the depth of the total real central potential:

We determine the depth from “(14)”, at $r = 0$,

Assumption that the Hatree-Fock term has a Wood-Saxon radial shape with energy-independent geometrical parameters (r_{HF}, a_{HF}) is given by

$$\mathcal{V}_{HF}(r, E) = \mathcal{V}_{HF}(E) f(r, R_{HF}, a_{HF}) \quad (25)$$

Where the depth $\mathcal{V}_{HF}(E)$ is given by the following parametrization:

$$\mathcal{V}_{HF}(E) = \mathcal{V}_{HF}(E_F) e^{[\alpha_{HF}(E - E_F) / \mathcal{V}_{HF}(E_F)]} \quad E \geq E_F \quad (26)$$

$$\mathcal{V}_{HF}(E) = \mathcal{V}_{HF}(E_F) + \alpha_{HF}(E - E_F) \quad E \leq E_F$$

Where α_{HF} , the slope parameter, $R_{HF} = r_{HF} A^{1/3}$, radius parameter, $\mathcal{V}_{HF}(E_F)$ is the depth at Fermi energy.

2.6. Volume Integral per Nucleon of the Real Potential

Determining the continuous energy variation of the volume integral per nucleon of the real potential:

The volume integral per nucleon of the real potential is given by:

$$[r^2]_V(E) = [r^2]_{HF}(E) + [r^2]_{\Delta V_W}(E) \quad (27)$$

Where $[r^2]_{HF}(E)$, the volume integral per nucleon of the Hartree-Fock that can be written as follows,

$$[r^2]_{HF}(E) = \mathcal{V}_{HF}(E) * g_{HF} \quad (28)$$

Where g_{HF} , is given by

$$g_{HF} = \frac{4\pi}{3} \frac{R_{HF}^3}{A_t A_p} \left[1 + \left(\frac{\pi \alpha_{HF}}{R_{HF}} \right)^2 \right] \quad (29)$$

2.7. Radius Parameter of the Total Real Central Potential

Determining the continuous energy variation of the radius parameter of the Woods-Saxon approximation to the full potential.

We determine the radius parameter of the Woods-Saxon approximation to the full optical potential from the equation:

$$R_V(E)^3 + (\pi a_V)^2 R_V(E) - \left(\frac{3}{4\pi} \right) g_V(E) A_t A_p = 0 \quad (30)$$

Where a_V , diffuseness parameter and $g_V(E)$, can be determined from the relation:

$$g_V(E) = [r^2]_V(E) / \mathcal{V}(E) \quad (31)$$

So, the radius parameter will be:

$$r_V(E) = R_V(E) A^{-1/3} \quad (32)$$

2.8. Comparing with the Global Parameterizations of the Optical Model Potential

After calculating the volume integral per nucleon of the mean field components, we have compared them with global parameterizations of the optical potential, in addition to calculating the depths and the geometrical parameters whose calculations have been performed in the (VMA) program:

1. Koning and Delaroche (Kd) [2], for

$$0.001 \leq E \leq 200 \text{ Mev}, Z_t = (12 - 83), A_t = (24 - 209)$$

2. Madland (Md) [11, 15], for

$$50 \leq E \leq 400 \text{ Mev}, Z_t = (6 - 82), A_t = (12 - 208)$$

3. Results and Discussion

The results According to the (VMA) and (SPI-GENOA) programs are summarized as follows:

3.1. Input Parameters

The values of the input parameters in the VMA program for the neutrons scattering by ⁶⁰Cu nucleus are showed in the (Table 1).

Table 1. The values of the input parameters.

Brown-Rho Parameters				
ρ_w, MeV	ρ_{wV}, MeV	$\beta, \text{MeV} \cdot \text{fm}^3$	$E_f \text{ (MeV)}$	
11.0	58.0	93.0	-10.8848128	
Geometrical Parameters				
a_v, fm	r_{wv}, fm	r_d, fm	a_{wv}, fm	a_d, fm
0.664	1.261	1.261	0.602	0.602
Hartree-Fock Parameters				
r_{HF}, fm	a_{HF}, fm	α_{HF}	$\mathcal{V}_{HF}(E_f), \text{MeV}$	
1.236	0.62	0.448	492.59	
(Spin-Orbit) term Parameters				
V_{SO}, fm	W_{SO}, fm	r_{SO}, fm	a_{SO}, fm	
6.8	0.0	1.2	0.6	
(Projectile-Target) Parameters				
Z_n	$A_n \text{ (amu)} [14]$	Z_t	$A_t \text{ (amu)} [14]$	
0.0	1.0086	29	59.594	

3.2. Volume Integrals per Nucleon of the Imaginary Parts of the Mean Field

The energy dependence of the volume integrals per nucleon of the imaginary parts of the mean fields are compared with these resulted from global parameterizations of the optical potential and with these resulting from the single fits of the potential parameters of the experimental data according to SPI program, within the energy range $(E_f - 120)\text{MeV}$, as they are showed in the Figure 1. From the figure it becomes clear for us: The energy dependence of the volume integrals per nucleon showed agreement in the behavior comparing with these resulted from global parameterization of the optical model potential, and fitting of these resulted from the single fits of the available experimental data.

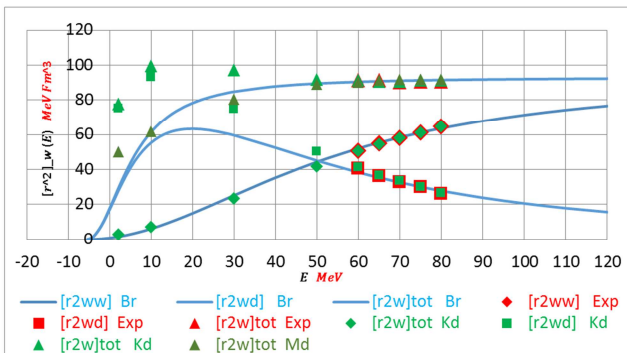


Figure 1. Volume integrals per nucleon of the imaginary parts of the mean field as a function of neutron energy (the red line) compared with these resulted from global parameterization of the optical model potential and with these resulted from the single fits of the potential parameters of the experimental data.

3.3. Depths of the Imaginary Parts of the Mean Field

The energy dependence of the depths of the (volume and surface) imaginary parts of the mean field within the energy range (from -100 to +100) MeV are showed in the Figure 2. From the figure we have observed a rapid variation of the depths in the vicinity of the Fermi energy and slowly variation toward the highly energies which are ascribed to a strong coupling between the elastic channel and the other reaction channels.

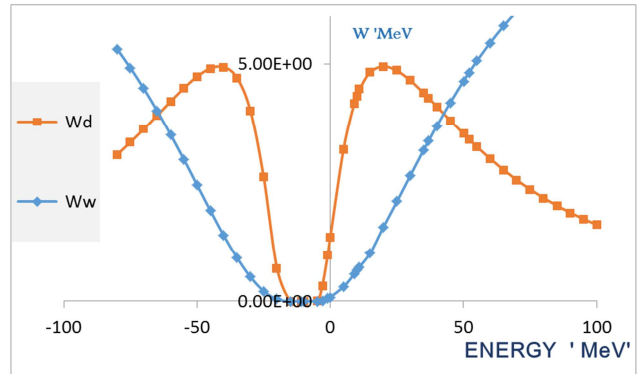


Figure 2. Depths of the (volume and surface) imaginary parts of the mean field as a function of neutron energy.

3.4. Volume Integral Per Nucleon of Total Dispersive Correction of the Real Part of the Mean Field

The energy dependence of the volume integral per nucleon of total dispersive correction of the real part of the mean field within the energy range from (-100 to +100) MeV is showed in the Figure 3.

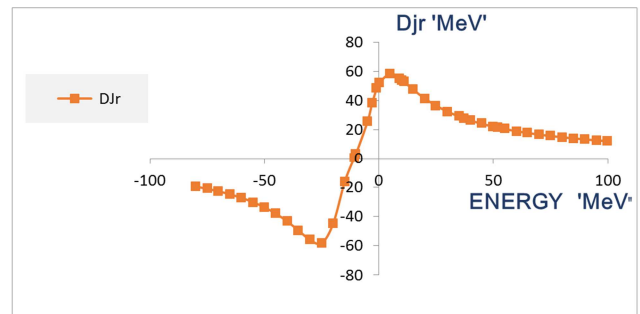


Figure 3. Volume integral per nucleon of total dispersive correction of the real part of the mean field as a function of neutron energy.

3.5. Volume Integral Per Nucleon of the Real Part of the Mean Field

The energy dependence of the volume integral per nucleon of the real part of the mean field obtained using dispersion relations with its HF approximation of the nonlocal potential for bound and unbound energies are compared with these resulted from global parameterizations of the optical potential and with these resulted from the single fits of the potential parameters of the experimental data [16] according to SPI program, as they are showed in the Figure 4.

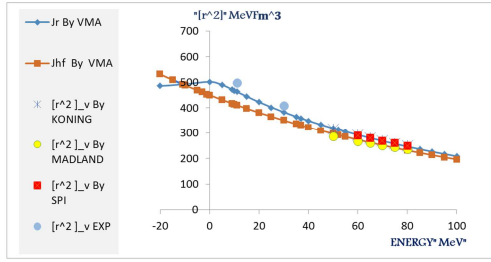


Figure 4. Volume integral per nucleon of the real part of the mean field as a function of neutron energy compared with these resulted from global parameterization of the optical model potential and with these resulted from the single fits of the potential parameters of the experimental data.

3.6. Depth of the Total Real Central Potential

The energy dependence of the depth of the total real central potential obtained by adding dispersion correction with its HF approximation of the nonlocal potential for bound and unbound energies are showed in the Figure 5. From the figure it becomes clear for us: The energy dependence behavior of both two potentials are the linear behavior according to the two following equations:

$$U_V(E) = -0.3233 E + 54.024 \quad (33)$$

$$U_{HF}(E) = -0.3914 E + 53.496 \quad (34)$$

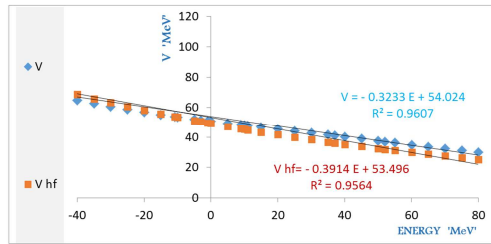


Figure 5. The energy dependence of the depth of the Wood-Saxon approximation to the mean field potential with its HF approximation.

3.7. The Real Radius Parameter of the Mean Field

The energy dependence of the real radius parameter of the Wood-Saxon approximation to the mean field potential within the energy range from -80 MeV to 110 MeV is showed in the Figure 6. From the figure we have observed a rapid variation of the real radius parameter (a characteristic wiggle) in the vicinity of the Fermi energy and then slow variation toward the high energies. This wiggle is thus due to a strong coupling between the elastic channel and the other reaction channels.

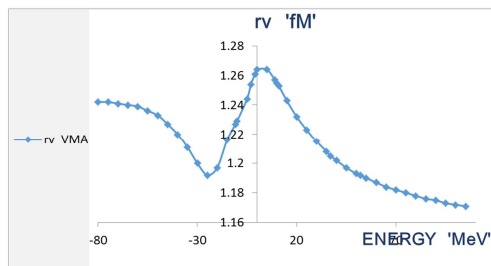


Figure 6. The energy dependence of the radius parameter of the Wood-Saxon approximation to the mean field potential with its HF approximation.

3.8. Cross Sections

The total cross section within the energy range (5 – 153) MeV is compared with these resulted from global parameterizations of the optical potential and with available experimental data [17, 18], and are (mb), as they are showed in the Figure 7. There is excellent agreement with the experimental data and the global parameterization of the optical potential according to our calculations in the (SPI-GENOA) program.

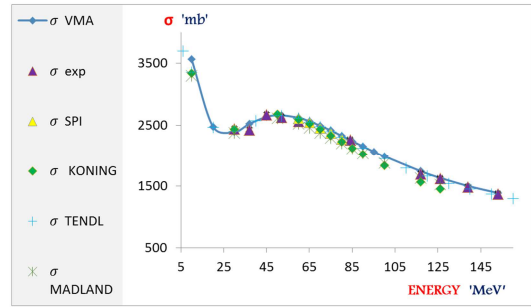


Figure 7. The energy dependence of the total cross section (the red line) compared with experimental value and with these resulted from global parameterization of the optical model potential.

4. Conclusion

The important conclusions can be shown as follows:

- i. Our analysis of the neutrons scattering by ^{60}Cu nucleus according to the variational moment approach drawn for certain input values of the mean field parameters.
- ii. Our calculation of the continuous energy variations of the volume integrals per nucleon of the imaginary parts of the mean fields showed an excellent agreement with these resulted from global parameterizations of the optical potential and with these resulted from the single fits of the potential parameters of the experimental total cross sections data.
- iii. Our calculation of the continuous energy variation of the depths of the (volume and surface) imaginary parts of the mean field for bound and unbound energies showed excellent agreement in the behavior (symmetric) in the vicinity of the Fermi energy.
- iv. Our calculation of the continuous energy variation of the volume integral per nucleon of the real part of the mean field obtained by adding dispersion correction with its HF approximation of the nonlocal potential for bound and unbound energies showed an excellent agreement with these resulted from global parameterizations of the optical potential and with these resulted from the single fits of the potential parameters of the experimental total cross sections data.
- v. Our calculation of the continuous energy variation of the depth of the real part of the mean field obtained by adding dispersion correction with its HF approximation of the nonlocal potential for bound and unbound energies showed the energy dependence behavior of both two potentials are the linear behavior according to

the two equations (33-34). In addition to continuous energy variation of the real radius parameter of the Wood-Saxon approximation to the mean field potential is a characteristic wiggle in the vicinity of the Fermi energy. This wiggle is thus due to a strong coupling between the elastic channel and the other reaction channels.

- vi. Our prediction of the total cross section data within the energy range (5 – 153) MeV showed excellent agreement with available experimental data.

References

- [1] Hodgson, P. E. (1990). The unification of the nuclear optical potential, *Contemporary Physics*, 31: 5, 295-308, DOI: 10.1080/00107519008213780.
- [2] Koning, A. J., & Delaroche, J. P. (2003). *Nucl. Phys. A*713, 231.
- [3] Mahaux, C., & Sartor, R. (1991). *Dispersion Relation Approach to the Mean Field and Spectral Functions of Nucleons in ^{40}Ca* , Nuclear Physics, A528, pp. 253-297, Elsevier Science Publishers B. V. (North-Holland).
- [4] IAEA, (2006). *Handbook for Calculations of Nuclear Reaction Data, RIPL-2*, IAEA in Austria, (Final report of a coordinated research project, IAEA-TECDOC-1506), pp. 47-69.
- [5] Melkanoff, M. A, Saxon, D. S, Jnodvik, J. S., & Cantor, D. G. (1961). A Fortran Program for Elastic Scattering Analyses with the Nuclear Optical Model, University of California Press Berkeley and Los Angeles, Retrieved August 24, 2009 [EBook #29784], online at www.gutenberg.org, p. 111.
- [6] Al-Mustafa, H., & Belal. A. (2019). Program Design for Analyzing the Optical Model of the (Coulomb - Nuclear) Interference Potential, *Journal of AL Baath University, Homs-Syria*, 41 (18), 71-102.
- [7] Al-Mustafa, H., & Belal. A. (2019). A Dispersive Optical Model Analysis of the Protons Scattering by Titanium Element Nucleus and Its Natural Isotopes, *Nuclear Science, Science PG*, 4 (4): 44-51, DOI:10.11648/j.ns.20190404.12.
- [8] Al-Mustafa, H., & Belal. A. (2020). A Dispersive Optical Model Analysis of the Neutrons Scattering by Titanium Element Nucleus and Its Natural Isotopes, *Nuclear Science, Science PG*, 5 (1): 1-7, DOI:10.11648/j.ns.20200501.11.
- [9] ROMANOVSKY, E. A., & BELAL, A., & MORZENA, L. R. (1993), *News. RAS, Phys*, Vol. 57, No. 10, P. 179.
- [10] ROMANOVSKY, E. A., & BOTROS, S., & SBASKIA, T., E. (1995), *News. RAS, Phys*, Vol. 57, No. 10, P. 179.
- [11] MADLAND, D. G. (1997). "Progress in the Development of Global Medium-Energy Nucleon-Nucleus Optical-Model Potential", *Proc. OECD/NEA Specialists Meeting on Nucleon-Nucleus Optical Model to 200 MeV*, Bruyeres-le-Ch[^]atel, France, 129.
- [12] Perey, F. (1975)- ("SPI-GENOA: An Optical Model Code"), unpublished.
- [13] Wapstra, A. H., & Gove, N. B. (1971). "Nuclear-reaction and separation energies", Oak Ridge National Laboratory, Oak Ridge, Tenn. 37830.
- [14] Audi, G., & Wapstra, A. H. (1995). The Isotopic Mass Data. *Nucl. Phys A. 595*, 409-480.
- [15] Young, P. G., (1994), Los Alamos National Laboratory "EXPERIENCE AT LOS ALAMOS WITH USE OF THE OPTICAL MODEL FOR APPLIED NUCLEAR DATA CALCULATIONS", (Report LA-UR-94-3104).
- [16] Jeukenne, J. P, & Mahaux, C (1986), "Dependence upon mass number and neutron excess of the real part of the proton optical potential for mass numbers ($44 \leq A \leq 72$)". *Phys.Rev.V.C34M P. P. 468-479*.
- [17] Taylor, A. E, & Wood, E. (1941), "Neutron total cross section between 30 and 153 MeV" *The London, Edinburgh, and Dublin Philosophical Magazine and Journal of Science, Series 7*.
- [18] TENDL-2019 Nuclear Data Library- Neutron sub-Library for Cu ($Z=29$) and ($A=60$) Tabular production and total cross sections, Elastic angular distribution.